

See discussions, stats, and author profiles for this publication at: <https://www.researchgate.net/publication/230593922>

# Development of double-decker pulse radiolysis

ARTICLE *in* THE REVIEW OF SCIENTIFIC INSTRUMENTS · JULY 2012

Impact Factor: 1.61 · DOI: 10.1063/1.4731652 · Source: PubMed

---

CITATIONS

4

---

READS

31

6 AUTHORS, INCLUDING:



**Koichi Kan**

Osaka University

40 PUBLICATIONS 117 CITATIONS

SEE PROFILE



**Jingan Yang**

Changzhou Institute of Technology

280 PUBLICATIONS 3,640 CITATIONS

SEE PROFILE



**A. Ogata**

Osaka University

142 PUBLICATIONS 904 CITATIONS

SEE PROFILE



**Yoshihito Yoshida**

St. Marianna University School of Medicine

852 PUBLICATIONS 9,291 CITATIONS

SEE PROFILE

## Development of double-decker pulse radiolysis

K. Kan, T. Kondoh, J. Yang, A. Ogata, K. Norizawa et al.

Citation: *Rev. Sci. Instrum.* **83**, 073302 (2012); doi: 10.1063/1.4731652

View online: <http://dx.doi.org/10.1063/1.4731652>

View Table of Contents: <http://rsi.aip.org/resource/1/RSINAK/v83/i7>

Published by the AIP Publishing LLC.

---

### Additional information on Rev. Sci. Instrum.

Journal Homepage: <http://rsi.aip.org>

Journal Information: [http://rsi.aip.org/about/about\\_the\\_journal](http://rsi.aip.org/about/about_the_journal)

Top downloads: [http://rsi.aip.org/features/most\\_downloaded](http://rsi.aip.org/features/most_downloaded)

Information for Authors: <http://rsi.aip.org/authors>

## ADVERTISEMENT

**physicstoday**

**Comment on any  
*Physics Today* article.**

**Measured energy in Japan**  
David von Seggern  
(vonneg@seismo.unr.edu) University of Nevada  
July 2012, page 10  
DIGITAL OBJECT IDENTIFIER  
<http://dx.doi.org/10.1063/PT.3.1619>  
The article by Thorne Lay and Hiroo Kanamori is an excellent review of the 1994 Chilean earthquake.

**Comment on this article**  
By the act of hitting a ball with a bat, one calculates the force energy to deliver the ball to its new location, but one must also take into account that the ball extended its energy release to that which became struck by the ball as its momentum ceased and passed energy to the struck ball. Therefore the parameters of the damage extend into the future when the received energy to that pushed upon, later becomes released in a new event. Perhaps calculations of one added that in, while another's calculations did not. E.M.C.  
Written by Edgar McCarroll, 14 July 2012 19:59

## Development of double-decker pulse radiolysis

K. Kan,<sup>a)</sup> T. Kondoh, J. Yang, A. Ogata, K. Norizawa, and Y. Yoshida

*Institute of Scientific and Industrial Research, Osaka University, Osaka, Japan*

(Received 2 May 2012; accepted 10 June 2012; published online 6 July 2012)

Double-decker pulse radiolysis (DDPR), which utilizes double-decker electron beams, was investigated to develop a new pulse radiolysis with a high time resolution. The double-decker electron beams were generated by injecting two UV pulses into a photocathode radio-frequency gun. In the pulse radiolysis, one electron beam was used as a pump beam, and the other was converted to a probe pulse. Finally, as its first application, the DDPR was successfully used for observing solvated electrons in water, with a 10%–90% rise time of 8.6 ps. © 2012 American Institute of Physics. [<http://dx.doi.org/10.1063/1.4731652>]

### I. INTRODUCTION

Pulse radiolysis,<sup>1,2</sup> which utilizes a pump electron beam and a probe pulse, is a powerful tool that can be used for the observation of ultrafast radiation-induced phenomena involving the mechanical motion of electrons and atomic nuclei in reaction mechanisms that are studied in physics, chemistry,<sup>3–5</sup> and biology.<sup>6</sup> In the 1960s, the first picosecond pulse radiolysis<sup>1</sup> was developed at the University of Toronto using an electron bunch train produced by an S-band accelerator. Since then, several studies on picosecond pulse radiolysis have been performed at Argonne National Laboratory,<sup>2</sup> the University of Tokyo,<sup>7</sup> and Osaka University.<sup>8</sup> In 2000, a sub-picosecond pulse radiolysis was developed by a group at Osaka University using an electron beam from an L-band accelerator and a probe pulse from a synchronized femtosecond laser.<sup>9</sup> Recently, several groups at Brookhaven National Laboratory,<sup>10,11</sup> the University of Paris-Sud,<sup>12</sup> the University of Tokyo,<sup>13</sup> and Osaka University<sup>5</sup> have studied pulse radiolysis using a probe pulse from a laser and a photocathode radio-frequency (RF) gun accelerator that is driven by a laser. Pulse radiolysis with a high time resolution, which will be developed in the future, would give a more comprehensive understanding of ultrafast phenomena not only for monitoring but also for controlling radiation-induced phenomena. However, the time resolution of pulse radiolysis is limited by the pulse widths of the electron beam (pump source) and the probe pulse, the difference in their velocities due to the refractive index of the sample, and the synchronized time jitter between them.<sup>5</sup>

At Osaka University, a photocathode-based linear accelerator (linac) and a magnetic bunch compressor were constructed for femtosecond pulse radiolysis based on a femtosecond electron bunch.<sup>14–16</sup> In the linac, a picosecond electron beam was generated using a photocathode RF gun and a Nd:YLF picosecond UV laser as a driving laser. The picosecond electron beam was accelerated up to 32 MeV by a booster linac with an optimal energy-phase correlation for compression. Finally, the electron bunch was successfully compressed into femtoseconds, e.g., 98 fs in rms at 0.2 nC.<sup>14</sup> As a result, the combination of a femtosecond electron beam

and a femtosecond laser realized pulse radiolysis with femtosecond time resolution, e.g., ~230 fs, due to the femtosecond pulse widths of both.<sup>4,5</sup> For improving the synchronized time jitter between a pump beam and probe pulse, double-decker electron beams were used as the pump beam and probe pulse; the double-decker beams were generated using two UV pulses from the driving laser.<sup>17</sup> Double-decker pulse radiolysis (DDPR) based on these beams would improve the synchronized time jitter because it would preclude RF synchronization between a pump electron beam and a probe laser.

In this paper, DDPR, which utilizes double-decker electron beams, was investigated for developing a new pulse radiolysis with a high time resolution. The double-decker electron beams were generated by two UV pulses and a photocathode RF gun for use as the pump beam and probe pulse in the pulse radiolysis measurement.

### II. EXPERIMENTAL ARRANGEMENT

Figure 1 shows the DDPR setup, including the laser injection system, the photocathode RF gun linac, and the pulse radiolysis system from upstream. In the laser injection system, a Nd:YLF picosecond laser was used to drive the photocathode. The output of the picosecond laser was 200  $\mu$ J/pulse of UV pulse (262 nm) at 10 Hz. The FWHM pulse width of the UV light pulse was measured to be 5 ps using a femtosecond streak camera. The UV pulse was separated by a beam splitter (BS) to generate the double-decker electron beams. The temporal separation of the two UV pulses was adjusted by an optical delay (OD1). The interval of the two pulses was set to 4.2 ns, which corresponded to 12 periods of S-band RF (2.856 GHz, 1 period = 0.35 ns) because the double-decker electron beams should be accelerated by a similar electric field. Furthermore, the spatial separation was also adjusted by mirrors with actuators. The two UV pulses were directed to the photocathode RF gun linac. The linac system consisted of a 1.6-cell S-band RF gun with a copper cathode, a 2-m-long traveling-wave linac, and a magnetic bunch compressor; the details of the linac are discussed in Refs. 14–16. In order to generate the double-decker electron beams, the two UV pulses were injected into the photocathode. The incident angle of the UV pulses was ~68° with respect to the direction of the

<sup>a)</sup>koichi81@sanken.osaka-u.ac.jp.

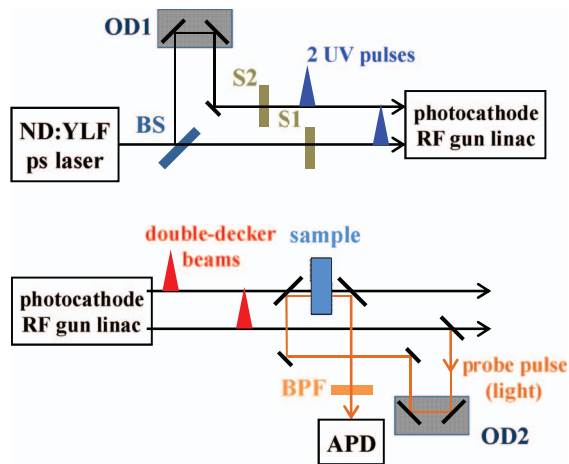


FIG. 1. (Top) Laser injection system and (bottom) pulse radiolysis system in the DDPR. BS denotes a beam splitter; S, a shutter; OD, an optical delay; BPF, a band-pass filter; and APD, a silicon avalanche photodiode.

electron beam, and this angle was chosen to increase the beam charge. The incident angle enhanced the bunch charge due to a polarization effect on the copper cathode.<sup>18</sup> In this RF gun, the enhancement factor of the bunch charge due to the polarization effect at  $68^\circ$  incident angle was found to be  $\sim 5$  compared with that at  $2^\circ$  incident angle. The UV pulses on the cathode were arranged almost horizontally because the double-decker electron beams were rotated azimuthally due to a longitudinal magnetic field of a solenoid magnet at the gun exit. The double-decker electron beams were accelerated in the gun and the linac using a 35-MW klystron. The beam energy at the gun exit was  $\sim 4$  MeV at a laser injection phase of  $30^\circ$  according to a measurement using a dipole section and screen. In the linac, the electron beams were accelerated up to 32.7 MeV. A total beam charge of 1.4 nC was generated by a UV pulse of  $200 \mu\text{J}/\text{pulse}$  at a laser injection phase of  $30^\circ$ . In the experiment, the linac phase was set to  $85^\circ$  to minimize energy spread of the beams from the viewpoint of transportation. The beams traveled through the magnetic bunch compressor. The rms pulse widths of the double-decker beams were estimated to be  $\sim 1$  ps according to the linac phase condition.<sup>14</sup> Finally, the double-decker electron beams were used in the pulse radiolysis system. The front electron beam of the double-decker beams was converted into a probe pulse by Cherenkov radiation in the air. The path length for the Cherenkov radiation was set to 280 mm to obtain sufficient light intensity, which depends on the path length.<sup>19</sup> The probe pulse traveled through an optical delay (OD2) in order to measure time-resolved transient absorption in the sample. The back electron beam, which was used as a pump electron beam, reached the sample with a delay of 4.2 ns with respect to the front beam. The probe pulse was injected into the sample after it had traveled a long path. The spatial distance between the paths for Cherenkov radiation and the pump beam was set to  $\sim 5$  mm in the vertical direction to avoid the beam used as the probe pulse from traveling through mediums, e.g., the mirrors and sample, as shown in Fig. 1. The intensity of the probe pulse, which decreased due to transient absorption in the sample caused by the back beam, was monitored by a silicon avalanche photo-

diode (APD) (S2382, Hamamatsu Photonics K. K.) through an optical fiber. The APD was driven by a bias voltage of 60 V. The waveforms from the APD were measured by an oscilloscope (6100A, LeCroy Co.). Spectral information of the absorption was selected by a band-pass filter (BPF) (FKB-VIS-40, Thorlabs). Shutters (S1/S2) controlled the generation of the front/back electron beams for the probe/pump sources, respectively.

### III. RESULTS AND DISCUSSIONS

#### A. Generation of double-decker electron beams

Figure 2 shows the spatial and temporal separations of the double-decker electron beams. Figure 2(a) shows the spatial separation at the sample position measured by a screen. The distance between the beams was adjusted to  $\sim 5$  mm because of the geometry of the sample and conversion to the probe pulse with Cherenkov radiation. The spatial distances between the double-decker electron beams at the gun exit and at the linac exit were 7.8 and 6.6 mm, respectively. The distance was not constant, because the beams traveled through magnets and RF cavities, which focused or defocused the beams. The back (top)/front (bottom) electron beams were used for the pump/probe sources, respectively. Figure 2(b) shows the temporal separation measured by a current transformer (CT) at the gun exit. To adjust the temporal separation,

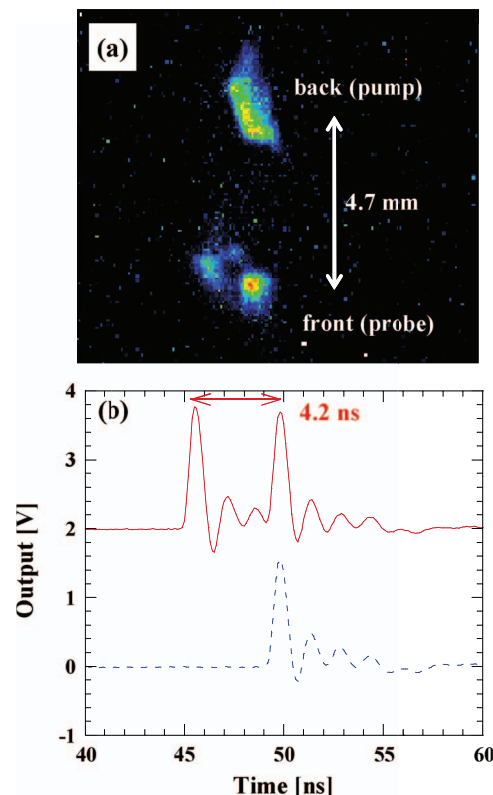


FIG. 2. (a) Spatial separation of the double-decker electron beams at the sample position. The back (top)/front (bottom) electron beams were used for the pump/probe sources, respectively. (b) Temporal separation at the gun exit with only the offsets adjusted for comparison. Waveforms for cases using two UV pulses (solid line) and using one UV pulse for the back beam (dotted line) are shown.



the energies of the beams at the linac exit were set to the same level by the optical delay (OD1) in the laser injection system. The beam energies were measured by a bending magnet and screen. The interval of the double-decker electron beams was measured to be 4.2 ns. The electron bunch charges were 0.74 nC (front) and 0.62 nC (back) according to the CT sensitivity of 0.35 nC/V peak-to-peak.

## B. First double-decker pulse radiolysis

Figure 3 shows the results of the first DDPR measurement. A water sample with a thickness of 10 mm was used. Figure 3(a) shows the photodiode outputs (peak-to-peak) as a function of the optical delay (OD2) in the pulse radiolysis system with a BPF of  $800 \pm 20$  nm. The BPF was set upstream from the optical fiber in order to select spectral information. Data for  $L$  and  $B$  denote the outputs for usage of only “Light” generated by Cherenkov radiation and only “Beam” from the pump source, respectively. Data for  $LB$  denote the output for the combination of  $L$  and  $B$ . Each data set corresponds to the conditions of the shutters in the laser injection system in Fig. 1. Briefly,  $LB$ ,  $L$ , and  $B$  denote the shutter conditions (S1/S2) for front/back electron beams of opened/opened, opened/closed, and closed/opened, respectively.

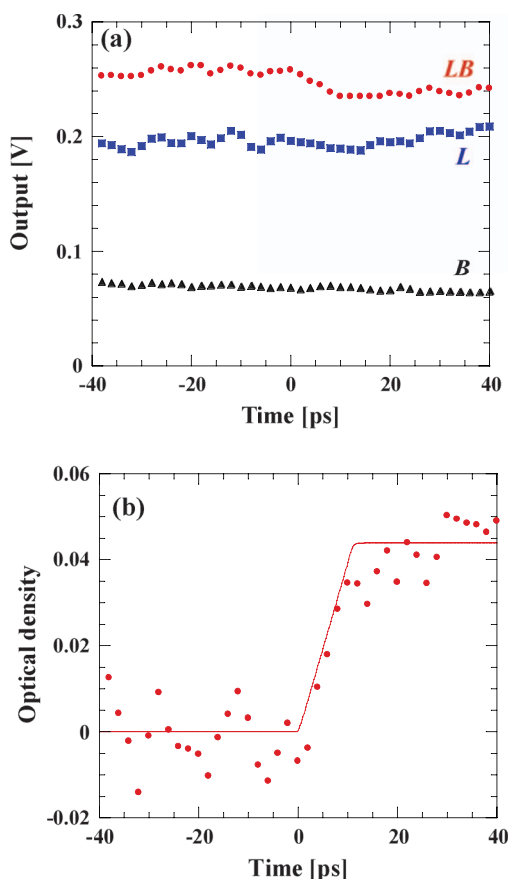


FIG. 3. (a) Photodiode outputs as a function of the optical delay in the pulse radiolysis system with a BPF of 800 nm.  $LB$ ,  $L$ , and  $B$  denote the shutters (S1/S2) conditions for front/back electron beams of opened/opened, opened/closed, and closed/opened, respectively. (b) Transient absorption due to the solvated electrons. Solid line denotes the simulation result using least-squares fitting.

tively. Each data set corresponds to the averaged value using 40 sweeps of the oscilloscope. Only when the probe pulse went through the sample following the pump beam was light absorbed due to the solvated electrons generated by the pump beam. As a result, the plot for  $LB$  decreased in a time of  $\sim 0$  ps because of the light absorption. The intensity for  $B$ , which corresponded to Cherenkov radiation from the pump beam in the sample, could not be ignored, because of the intensity for  $L$ . In evaluation of the transient absorption according to the Beer-Lambert law, the optical density was estimated as  $O.D. = \text{Log}(I_0/I) = \text{Log}[L/(LB - B)]$ , where  $I_0$  denotes the intensity of the probe pulse without the pump beam and  $I$  denotes the intensity with the pump beam. The terms ( $LB$ ,  $L$ , and  $B$ ) denote the photodiode outputs for the conditions mentioned above. Figure 3(b) shows the transient absorption due to the solvated electrons according to the equation. The data in Fig. 3(a) were used to calculate the O.D. Expectedly, the O.D. increased in a time of  $\sim 0$  ps. Thus, the first DDPR was demonstrated with an O.D. change of 0.043, although the 10%–90% rise time was obtained as 8.6 ps, which depended mostly on the sample thickness.<sup>5</sup>

To improve the time resolution in DDPR, optimizations of the double-decker electron beams and pulse radiolysis system are intended to be carried out. In the optimization of the electron beams, generation of femtosecond double-decker electron beams<sup>14,17</sup> is intended to be applied to the generation of a femtosecond probe pulse. As regards the optimization of the pulse radiolysis system, a gas cell for Cherenkov radiator would increase the intensity of the probe pulse according to Refs. 2 and 19, resulting in an improvement of the S/N ratio and time resolution when using reference measurement of the probe pulse<sup>20</sup> and a thin sample cell. The overlap between the pump electron beam and probe pulse should also be optimized according to the optical density reported in Ref. 5. At the same time, for improving the time resolution, which is limited by the difference in the velocities of the electron beam and the probe pulse, equivalent velocity spectroscopy (EVS) can be carried out. The use of an oblique electron beam in EVS has been shown to improve the time resolution of the pulse radiolysis compared with a case using a normal electron beam.<sup>21</sup> For improving the synchronized time jitter between a pump electron beam and a probe pulse, DDPR based on EVS would have the advantage of precise synchronization without RF synchronization, from which jitter is estimated to be  $\sim 60$  fs.<sup>5</sup> Optical systems used in DDPR would be more reliable for the jitter in terms of the precision of pump-probe measurements conducted using lasers. Because DDPR involves the use of a probe light based on an electron beam, it could be especially useful in cases where an electron beam of less than a few tens of femtoseconds<sup>16</sup> is generated. Application of the proposed pulse radiolysis in the terahertz (THz) range is also expected for detecting transient quasi-free electrons<sup>22</sup> because of THz-wave generation based on an electron beam.<sup>19,23</sup>

The optical systems of the proposed DDPR are more complicated than those of early pulse radiolysis<sup>2</sup> because of the generation and utilization of the double-decker electron beams. However, the early pulse radiolysis and DDPR are similar in that they both generate probe pulse using Cherenkov radiation. In early pulse radiolysis, a single

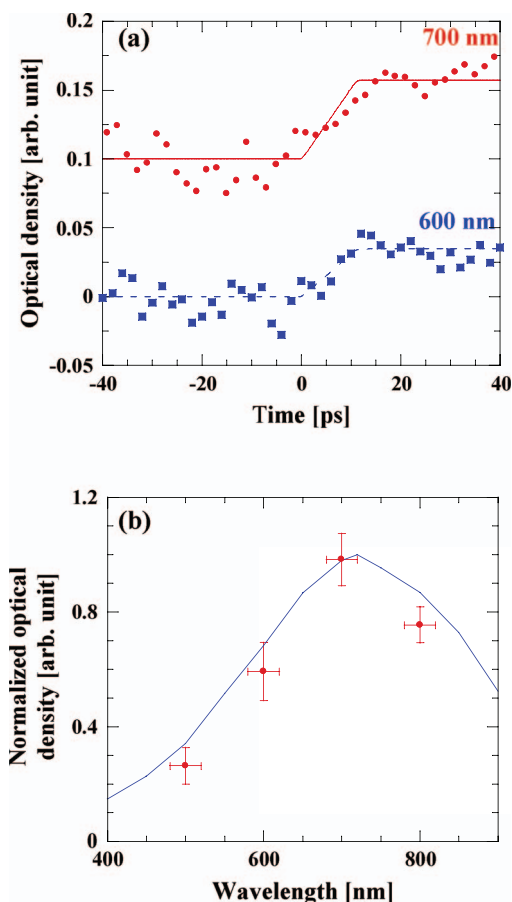


FIG. 4. Transient absorptions using BPFs of 700 nm (circles) and 600 nm (squares) with only offsets adjusted for comparison. Lines denote simulation results using least-squares fitting. (b) Comparison of spectra for solvated electrons in water measured by DDPR (circles) and nanosecond pulse radiolysis (solid line).

electron beam was used as a pump source after traveling through a Cherenkov cell<sup>2</sup> to produce a probe pulse. On the other hand, DDPR exploits a characteristic of the photocathode RF gun, which generates synchronized double-decker electron beams using a laser, although the bunch charge is lower than that in the early pulse radiolysis. The advantages of DDPR are due to the clear roles of the double electron beams with spatial and temporal separations. The pump beam is used only as the pump source of the sample. The scattering of the pump beam is minimized by designing the system such that the beam travels through the fewest mediums, e.g., the sample and mirrors, which is also the case in conventional pulse radiolysis using a probe pulse from a laser. The minimized scattering improves the density of solvated electrons and the bunch length degradation, resulting in improvements of the S/N ratio and time resolution in DDPR. For the probe pulse, the path length of Cherenkov radiation can be adjusted easily for the enhancement of intensity<sup>19</sup> due to a large air gap. The intensity of the probe pulse is most essential to pulse radiolysis because it is based on light absorption measurement. A large change in the path length requires a modification of the laser injection system according to the integral multiple of the accelerating RF. However, the flexibility in designing the probe pulse, including the use of a gas cell, would be impor-

tant for an experiment at a low bunch charge, which decreases the bunch length<sup>14,15</sup> due to the space-charge effect.

### C. Application to spectrum measurement

Figure 4 shows an application to a spectrum measurement using DDPR. The probe pulse in DDPR is white because of Cherenkov radiation. Figure 4(a) shows the transient absorptions using BPFs of  $700 \pm 20$  nm and  $600 \pm 20$  nm. The maximum change in optical density was observed in the case using a BPF of 700 nm because of the optical density peak for the solvated electrons in water at  $\sim 720$  nm.<sup>24</sup> Figure 4(b) shows the comparison of spectra for solvated electrons in water measured by DDPR and a nanosecond pulse radiolysis. The horizontal and vertical errors in DDPR corresponded to the bandwidths of the BPFs and stabilities of the O.D.s. Spectra for DDPR and nanosecond pulse radiolysis denote the optical densities at 30 ps and 2 ns after pump beam irradiation, respectively. The spectrum measured by DDPR agreed to that measured by a nanosecond pulse radiolysis, confirming the application of DDPR for spectrum measurement. In this case, the transient absorption was caused mainly by the solvated electrons in water; however, the BPF will be changed according to observed species.

## IV. CONCLUSIONS

Double-decker pulse radiolysis using double-decker electron beams was demonstrated, with a 10%–90% rise time of 8.6 ps. DDPR was also applied to spectrum measurement. In the future, the time resolution in DDPR is intended to be improved by generating femtosecond double-decker electron beams and optimizing various aspects of the pulse radiolysis system, e.g., the Cherenkov radiator, reference measurement, and EVS. Besides improving the time resolution, another application to a pulse radiolysis in THz-range would be expected.

## ACKNOWLEDGMENTS

We thank the staff of the Radiation Laboratory at the Institute of Scientific and Industrial Research (ISIR), Osaka University for the linac operation. This work was supported by KAKENHI (21226022).

<sup>1</sup>M. J. Bronskill, R. K. Wolff, and J. W. Hunt, *J. Phys. Chem.* **73**, 1175 (1969).

<sup>2</sup>C. D. Jonah, *Rev. Sci. Instrum.* **46**, 62 (1975).

<sup>3</sup>J. F. Wishart, S. I. Lall-Ramnarine, R. Raju, A. Scumpia, S. Bellevue, R. Ragbir, and R. Engel, *Radiat. Phys. Chem.* **72**, 99–104 (2005).

<sup>4</sup>T. Kondoh, J. Yang, K. Norizawa, K. Kan, and Y. Yoshida, *Radiat. Phys. Chem.* **80**, 286 (2011).

<sup>5</sup>J. Yang, T. Kondoh, K. Kan, and Y. Yoshida, *Nucl. Instrum. Methods A* **629**, 6 (2011).

<sup>6</sup>K. Kobayashi, M. Tsubaki, and S. Tagawa, *J. Biol. Chem.* **273**, 16038 (1998).

<sup>7</sup>Y. Tabata, H. Kobayashi, M. Washio, S. Tagawa, and Y. Yoshida, *Radiat. Phys. Chem.* **26**, 473 (1985).

<sup>8</sup>S. Takeda, K. Tsumori, N. Kimura, T. Yamamoto, T. Hori, T. Sawai, J. Ohkuma, S. Takamuku, T. Okada, K. Hayashi, and M. Kawanishi, *IEEE Trans. Nucl. Sci.* **NS-32**, 3219 (1985).

- <sup>9</sup>T. Kozawa, Y. Mizutani, M. Miki, M. Yamamoto, S. Suemine, Y. Yoshida, and S. Tagawa, *Nucl. Instrum. Methods A* **440**, 251 (2000).
- <sup>10</sup>J. F. Wishart, A. R. Cook, and J. R. Miller, *Rev. Sci. Instrum.* **75**, 4359 (2004).
- <sup>11</sup>A. R. Cook and Y. Shen, *Rev. Sci. Instrum.* **80**, 073106 (2009).
- <sup>12</sup>J.-L. Marignier, V. Waele, H. Monard, F. Gobert, J.-P. Larbre, A. Demarque, M. Mostafavi, and J. Belloni, *Radiat. Phys. Chem.* **75**, 1024 (2006).
- <sup>13</sup>Y. Muroya, X. Li, G. Wu, H. Ijima, K. Yoshi, T. Ueda, H. Kudo, and Y. Katsumura, *Radiat. Phys. Chem.* **72**, 169 (2005).
- <sup>14</sup>J. Yang, T. Kondoh, K. Kan, T. Kozawa, Y. Yoshida, and S. Tagawa, *Nucl. Instrum. Methods A* **556**, 52 (2006).
- <sup>15</sup>K. Kan, J. Yang, T. Kondoh, K. Norizawa, and Y. Yoshida, *Nucl. Instrum. Methods A* **597**, 126 (2008).
- <sup>16</sup>K. Kan, J. Yang, T. Kondoh, K. Norizawa, A. Ogata, T. Kozawa, and Y. Yoshida, *Nucl. Instrum. Methods A* **622**, 35 (2010).
- <sup>17</sup>J. Yang, T. Kondoh, A. Yoshida, and Y. Yoshida, *Rev. Sci. Instrum.* **77**, 043302 (2006).
- <sup>18</sup>E. Pedersoli, F. Banfi, B. Ressel, S. Pagliara, C. Giannetti, G. Galimberti, S. Lidia, J. Corlett, G. Ferrini, and F. Parmigiana, *Appl. Phys. Lett.* **87**, 081112 (2005).
- <sup>19</sup>T. Takahashi, T. Kanai, Y. Shibata, K. Ishi, M. Ikezawa, T. Nakazato, M. Oyamada, S. Urasawa, T. Yamakawa, K. Takami, T. Matsuyama, K. Kobayashi, and Y. Fujita, *Phys. Rev. E* **50**, 4041 (1994).
- <sup>20</sup>J. Yang, T. Kondoh, T. Kozawa, Y. Yoshida, and S. Tagawa, *Radiat. Phys. Chem.* **75**, 1034 (2006).
- <sup>21</sup>J. Yang, T. Kondoh, K. Norizawa, Y. Yoshida, and S. Tagawa, *Radiat. Phys. Chem.* **78**, 1164 (2009).
- <sup>22</sup>E. Knoesel, M. Bonn, J. Shan, and T. F. Heinz, *Phys. Rev. Lett.* **86**, 340 (2001).
- <sup>23</sup>K. Kan, J. Yang, A. Ogata, T. Kondoh, K. Norizawa, and Y. Yoshida, *Appl. Phys. Lett.* **99**, 231503 (2011).
- <sup>24</sup>G. Wu, Y. Katsumura, Y. Muroya, X. Li, and Y. Terada, *Chem. Phys. Lett.* **325**, 531 (2000).